Clays and Clay Minerals, Vol. 66, No. 2, 173–189, 2018.

REFLECTANCE SPECTROSCOPY OF ORGANIC MATTER IN SEDIMENTARY ROCKS AT MID-INFRARED WAVELENGTHS

H. H. KAPLAN* AND R. E. MILLIKEN

Department of Earth, Environmental, and Planetary Sciences, Brown University, 324 Brook St., Box 1846, Providence, RI, USA 02912

Abstract—Reflectance spectroscopy is a rapid, non-destructive technique capable of characterizing mineral and organic components within geologic materials at spatial scales that range from μm to km. The degree to which reflectance spectra can be used to provide quantitative information about organic compounds remains poorly understood, particularly for rocks with low organic content that are common in the Earth's ancient rock record and that may be present on other planetary bodies, such as Mars. In the present study, reflectance spectra (0.35−25 μm) were acquired for a suite of Proterozoic shales and the kerogen was isolated to assess how spectral properties of aliphatic and aromatic C-H absorption bands can be used to predict organic matter abundance (total organic content, TOC, and H/C ratio). A number of spectral parameters were evaluated for organic absorption bands observed in the 3−4 μm wavelength region for comparison with independently measured TOC and H/C values. Ratios of the strengths of aliphatic to aromatic absorption bands were directly correlated to H/C values, but the reflectance spectra for pure kerogens with H/C < 0.2 lacked clear evidence for C-H absorption bands in this spectral region. Organic absorption bands are routinely observed for bulk rock powders with >1 wt.% TOC, but the detection limits of reflectance spectra for TOC may be <1 wt.% or as high as 10 wt.%. Organic detection limits for reflectance spectra are, thus, controlled by both TOC and H/C values, but these parameters can be predicted for clay-rich, kerogen-dominated samples for a range of values that are relevant to drill cores, outcrops, meteorites, and planetary surfaces.

Key Words—Detection Limit, Organics, Reflectance, Sedimentary, Spectroscopy.

INTRODUCTION

Reflectance spectroscopy is a rapid and non-destructive technique that has been instrumental in deciphering the surface composition of Earth, Mars, the Moon, and other planetary bodies by its use on orbiters, landers, and rovers. In addition to planetary-scale exploration, the ability of visible to near-infrared and mid-infrared wavelength (VIS-NIR-MIR, ~0.5 to 25 μm or 20,000−400 cm^{-1}) reflectance spectroscopy to simultaneously detect mineralogy and organic matter has led to significant interest in this method for a wide range of geological applications. Reflectance measurements have been used to determine the mineralogical composition of terrestrial soils (*e.g.* Reeves, 2010), sedimentary rocks (*e.g.* Greenberger *et al*., 2015), rock powders (*e.g.* Craddock *et al*., 2017), lake and fluvial sediments (*e.g.* Goudge *et al*., 2017), and drill cores (*e.g.* Speta *et al*., 2016) to name a few. Other studies have compiled spectral libraries of organic compounds to catalog diagnostic absorption bands in reflectance data (*e.g.* Clark *et al*., 2009; Izawa *et al*., 2014) and several studies have attempted to quantify the organic contents of soils and geologic materials based on partial least squares or principal component regression of the reflectance spectra (*e.g.* Chang *et al*., 2001; Breen *et al*., 2008). Despite the growing number of applications, the utility of NIR-MIR reflectance spectroscopy for the quantitative analysis of total organic carbon (TOC) and H/C ratios of the organic materials in bulk rocks or rock powders remains largely unexplored, particularly for geologic samples with low TOC values that are relevant to studies of the ancient terrestrial rock record (*e.g.*, Proterozoic rocks) and planetary materials (*e.g.*, carbonaceous chondrite meteorites).

In the present study, NIR-MIR reflectance spectra of bulk sedimentary rock powders and the kerogens that were isolated from those powders were analyzed to address these questions. This work builds on a previous study of well-controlled synthetic mixtures of clay and organic compounds (Kaplan and Milliken, 2016) in order to better understand how those results compare with reflectance spectra of natural organic-bearing sedimentary rocks. The primary goal of the present study was to find spectral parameters that relate to organic composition and abundance for clay-rich (primarily illite) samples that have low TOC and for which the organic component is dominated by insoluble organic matter (kerogen). A secondary objective was to assess detection limits of organic materials in reflectance spectra with diagnostic absorption bands in the ~2−4 μm (5000−2500 cm^{-1}) wavelength region. Reflectance spectroscopy is hypothesized to be capable of identifying and extracting quantitative information about

* E-mail address of corresponding author:
Hannah_Kaplan@brown.edu
DOI: 10.1346/CCMN.2018.064092

organic material in low-TOC rocks in the geologic record of Earth and other planetary bodies. This hypothesis was tested and detection limits were assessed through analysis of the spectral parameters of well-characterized organic-bearing samples.

The position and strength of absorption bands in NIR-MIR reflectance spectra, spectral modeling, and statistical modeling were explored as potential methods to provide qualitative and/or quantitative estimates of TOC and H/C from the spectra of bulk rock powders. In addition to terrestrial applications, the results for these clay-bearing rocks with low TOC values may also provide an important foundation for understanding how reflectance spectroscopy can be used to rapidly detect and quantify properties of organic compounds in extraterrestrial materials. This could include laboratory studies of carbonaceous chondrite meteorites altered in contact with water, the application to remotely acquired reflectance data of C-type asteroids from satellite-based spectrometers, or the analysis of spectral data acquired by future rover-based measurements of rocks on Mars.

BACKGROUND

Applications of reflectance spectroscopy for organic detection

The use of reflectance spectroscopy, including VIS-NIR imaging spectroscopy, to simultaneously quantify mineral and organic components in natural materials has greatly increased in the last decade, with the majority of applications in soil science (Calderón *et al*., 2013; Nocita *et al*., 2014) and drill core analysis for hydrocarbon exploration (Herron *et al*., 2014; Washburn *et al*., 2015; Craddock *et al*., 2017). A wide range of VIS-NIR-MIR point and imaging spectrometers are now available through multiple vendors, including equipment, integrated packages, and for-fee services for using reflectance spectroscopy as a tool for core logging and mineral mapping (Herron *et al*., 2014; Speta *et al*., 2015; Mehmani *et al*., 2017). Recent publications that detail the application of reflectance spectroscopy to oil shales, and mapping of the organic content and mineralogy of drill cores in particular, suggests a potential increase in the use of NIR-MIR reflectance spectroscopy in the analysis of hydrocarbon reservoirs (van der Meijde *et al*., 2013; Chen *et al*., 2014; Herron *et al*., 2014; Craddock *et al*., 2017; Mehmani *et al*., 2017). Additional technological advancements, specifically in the development of cost-effective NIR-MIR imaging spectrometers, have the potential to expand these methods to a wider range of geologic applications that can include the detection and identification of organic compounds in the ancient terrestrial rock record *via* spectral mapping of drill cores, hand samples, and outcrops.

Reflectance spectroscopy at NIR-MIR wavelengths is also used in the search for organic compounds beyond Earth, where data are acquired by measuring solar radiation reflected from planetary surfaces or by active illumination of a target. Data will soon be returned from several planetary missions that are searching for organics using spectrometers that measure reflectance in the 3 − 5 μm wavelength range. The MicrOmega instrument, a hyperspectral microscopic imaging spectrometer, is onboard the Mobile Asteroid Surface Scout (MASCOT) lander on the Hayabusa2/MASCOT mission that is currently headed to Ryugu, a C-type asteroid that may host organic compounds (Pilorget and Bibring, 2013; Bibring *et al*., 2017). The MicrOmega spectrometer has also been chosen as part of the European Space Agency (ESA) ExoMars rover mission that is expected to launch in 2020 (Leroi *et al*., 2009; Bibring *et al*., 2017). NASA's Origins, Spectral Interpretation, Resource Identification, Security, Regolith Explorer (OSIRIS-REx) mission is currently en route to the asteroid Bennu and includes the Visible and InfraRed Spectrometer (OVIRS) instrument, which is a point spectrometer that will facilitate compositional mapping of the asteroid surface and organic detection; sample site selection will start in August 2018 (Reuter and Simon-Miller, 2012; Reuter *et al*., 2018).

Previous planetary instruments that have acquired reflectance data at NIR wavelengths and detected possible organic compounds include the Visible and InfraRed Thermal Imaging Spectrometer (VIRTIS) on ESA's Rosetta mission and a similar instrument on NASA's Dawn mission (where it is called 'VIR') (Coradine *et al*., 1998: Coradina *et al*., 2007; DeSanctis *et al*., 2017). The Cassini Visual and Infrared Mapping Spectrometer (VIMS) and Galileo Near-Infrared Mapping Spectrometer (NIMS) instruments also fit the spectral requirements. Both VIMS and NIMS traveled to the outer solar system and observed organic compounds (*e.g*. McCord *et al*., 2006; Cruikshank *et al*., 2014).

Ground-based spectra of asteroid 24 Themis revealed spectral features between 2 and 4 μm that are associated with ice and organics (Rivkin and Emery, 2010). Additional observations of organic compounds on planetary surfaces include the presence of a broad absorption feature that spans 2.9−3.6 μm in VIRTIS spectra for the comet 67P/Churyumov-Gerasimenko, which was interpreted as cometary organic macromolecular material (Capaccioni *et al*., 2015; Quirico *et al*., 2016). More recently, reflectance spectra of the dwarf planet 1 Ceres acquired by the Dawn VIR instrument were interpreted to indicate the presence of aliphatic organic compounds at the Cerean surface based on absorption bands near 3.4 μm (De Sanctis *et al*., 2017). In all of these cases, the amount and maturity of the organic material remains poorly constrained, which is primarily due to a fundamental lack in knowledge of how best to derive quantitative information from reflectance spectra for organic compounds that are

https://doi.org/10.1346/CCMN.2018.064092 Published online by Cambridge University Press

intimately mixed with inorganic phases.

In summary, VIS-NIR-MIR reflectance spectra capable of identifying organic matter in geologic materials and settings have been and will continue to be acquired for Earth and beyond in the coming years. The increasing availability of imaging spectrometers and their use in the field, laboratory, and on airborne platforms allows for the acquisition of reflectance data over a wide range of spatial scales while maintaining spatial context, which is an important aspect for many geological applications (*e.g.* Greenberger *et al*., 2015). The ongoing acquisition and analysis of such data necessitates an experimental and theoretical underpinning of how to extract accurate quantitative information on organic material in these settings that includes estimates of TOC and H/C values. This study examined the constraints and quantitative capabilities of reflectance spectroscopy in this context for a set of conditions that are relevant to studies of the ancient Earth and extraterrestrial materials, such as clay-bearing rocks with low total organic contents that are dominated by insoluble organic matter (*i.e*., kerogen).

Spectral Reflectance Characteristics of Organic-Bearing Materials

In reflectance spectroscopy, the complex effects of multiple scattering (where a photon interacts with multiple particles before being scattered to a detector), non-linear effects of particle size (Mustard and Hays, 1997), and albedo (Nash and Conel, 1974; Milliken and Mustard, 2007) make quantification of absorbing species difficult in comparison to other spectroscopic techniques, such as transmission spectroscopy. In addition, not all vibrational modes in organic materials are IR active and techniques such as Raman spectroscopy may be sensitive to a wider range of organic compounds. Reflectance spectroscopy may be advantageous in that it is rapid, requires no or minimal sample preparation, is non-destructive, and the data can be directly compared with reflectance spectra that are commonly measured using airborne, satellite, and lander/rover systems.

Qualitative and quantitative analyses of reflectance spectra commonly require the creation of high quality spectral libraries for well-characterized samples. With respect to organic compounds, a comprehensive spectral library of polycyclic aromatic hydrocarbons has been compiled with the position of VIS-NIR absorption bands identified for astrophysical and planetary applications (Izawa *et al*., 2014). A similar spectral library of alkanes was assembled by Clark *et al*. (2009), which has been used to identify organic compounds on Saturn's moon Titan (Clark *et al*., 2010). NIR spectral properties have also been examined for a variety of carbon-bearing materials from graphite to oil sands for remote sensing applications (Cloutis *et al*., 1994; Rivard *et al*., 2010). Reflectance spectroscopy of pure organic compounds has limited applications outside of a laboratory setting and studies that examine the organics that are hosted within an inorganic matrix (*e.g*., sedimentary rocks) are warranted to better understand the benefits and limitations of reflectance spectroscopy as a quantitative tool for organic detection.

Aliphatic C-H bonds in CH_2 and CH_3 groups give rise to three distinct absorption bands near 3.3–3.6 μm (~3000–2800 cm^{-1}), *i.e*. a spectral 'triplet' (Figure 1). Aromatic C-H absorption bands occur at slightly shorter wavelengths (3.1–3.3 μm, or ~3225–3000 cm^{-1}), though this absorption band is commonly much weaker than the aliphatic triplet when observed in reflectance spectra (Figure 1). At longer wavelengths, absorption bands due to C-O, C-C, and C=C are found. Although some of these absorption bands can arise from inorganic compounds, these absorption bands will be referred to as 'organic absorption bands' here for simplicity and exceptions are noted below in the discussion section.

Spectral analysis of organic absorption features

A number of methods have been developed to interpret reflectance spectra in terms of the presence and amount of an absorbing component. The simplest of these is band depth, which measures the strength of an absorption band by finding the distance between the absorption maximum (reflectance minimum) and a spectral continuum or baseline. Clark and Roush (1984) defined band depth as: $D(\lambda) = 1 - R_b(\lambda)/R_c(\lambda)$, where R_b is the reflectance value at the maximum absorption point and R_c is the reflectance value of the user-defined continuum slope at the same wavelength, λ (*i.e*., the reflectance value that would likely be observed at that wavelength in the absence of an absorption band).

Band depth and other spectral parameters have previously been applied to the study of kerogens and organic-bearing sedimentary rocks. IR spectroscopy of kerogen and bitumen has been used to link specific absorption bands to H/C or organic maturity as independently estimated by vitrinite (*i.e*. vitreous alteration product of lignin and cellulose in coal) reflectance (*e.g*. Chrisy *et al*., 1989; Ganz and Kalkreuth, 1991; Lis *et al*., 2005; Rivard *et al*., 2010). More recently, Craddock *et al*. (2017) found that organic absorption strength was correlated to both kerogen content and maturity of mudrocks and they defined a maturity-based scaling factor in order to predict type II kerogen contents in mudrocks. The H/C ratio of kerogen is known to decrease with maturity, even though the carbon content remains the same. The reflectance spectrum in the 3–4 μm region is most sensitive to H in kerogen rather than C and so changes in maturity are reflected in the spectrum. Craddock *et al*. (2017) modeled absorption bands using a polynomial fit to analyze spectral amplitude instead of direct band depth values. Other studies have used Gaussian and Lorentzian curve fitting techniques to interpret the reflectance spectra of pyroxene and olivine minerals (*e.g*.

https://doi.org/10.1346/CCMN.2018.064092 Published online by Cambridge University Press

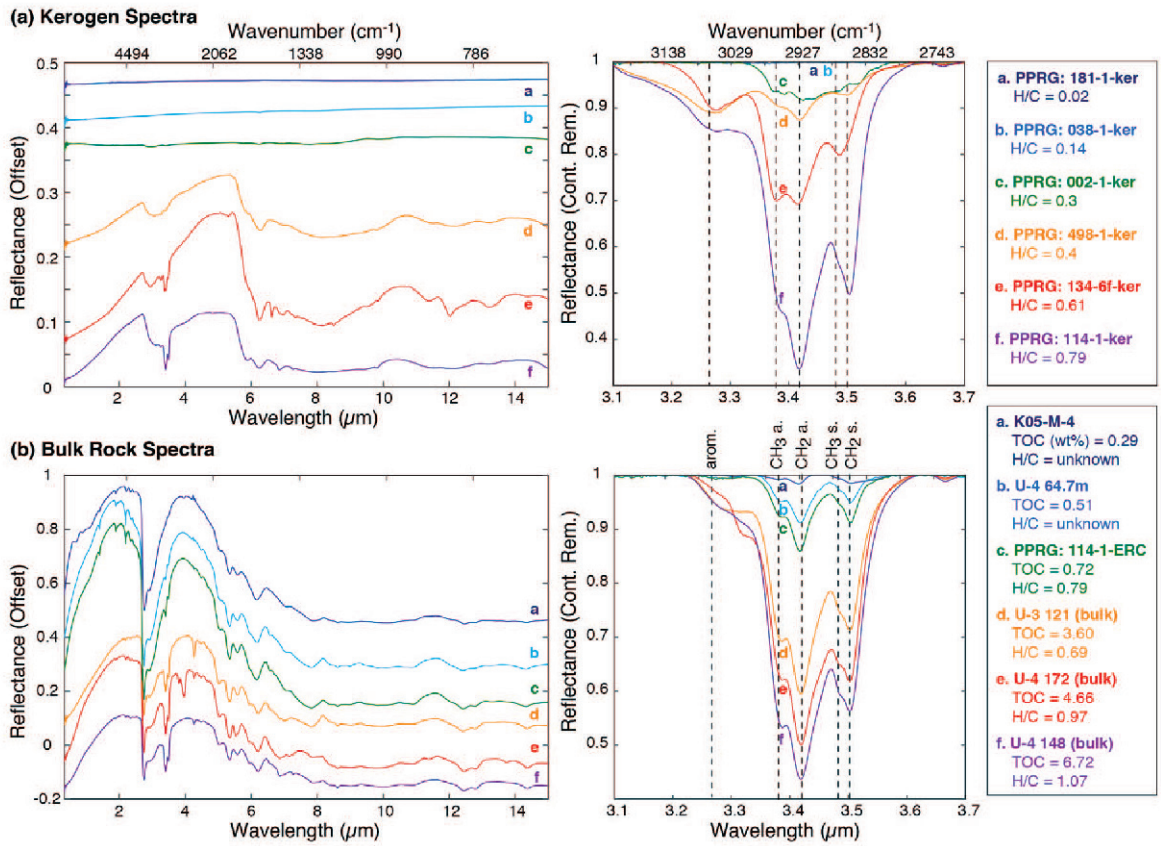

Figure 1. Reflectance spectra of select (a) kerogen separates and (b) bulk rocks. Full spectra (0.35 – 15 μm) and continuum-removed spectra (3.1 – 3.8 μm) are displayed on the left and right side plots, respectively, with major absorption bands labeled (a – asymmetric, s – symmetric stretches). The available H/C and TOC values are given along with the sample names.

Sunshine and Pieter, 1993) and this method has been used to investigate the composition of insoluble organic matter (IOM) in carbonaceous meteorites (Orthous-Daunay *et al*., 2013). Moroz *et al*. (1998) found that the wavelength position of a reflectance maximum near 2.2 μm corresponds to the aromaticity of C in bitumen and that the ratio of the reflectance values at 2.16 and 2.7 μm can be used to estimate the H/C ratio in the bitumen. These shorter wavelength (~2 μm) combination vibration bands, however, are much weaker than fundamental C-H vibration modes observed in the 3–4 μm wavelength region and are only commonly observed in the spectra of bright, organic-rich materials.

Other common spectral analysis techniques are statistical methods that use data at every wavelength in the reflectance spectrum rather than focusing on individual absorption bands linked to C-H vibrations. These techniques, which include partial least squares regression and principal component analysis, have been used to predict organic C in soils and reviews have been carried out on its applicability at different wavelength ranges (NIR *vs*. MIR) and in laboratory *vs.* field settings (McCarty *et al*., 2002; Reeves, 2010). MIR wavelengths (2.5–20 μm) lead to more successful predictions than NIR-wavelengths (1–2.5 μm) due to the presence of C-associated absorption bands (Reeves, 2010).

Despite these previous studies and direct observations of organic absorption bands in terrestrial and extra-terrestrial materials, little detailed information is available for specific variables that affect the reflectance spectra of organic-bearing rocks or rock powders and how these variables contribute to spectral absorption bands. Most previous studies (*e.g*. Chang *et al*., 2001; Washburn *et al*., 2015) used partial least squares or principal components analysis to quantify organics based on reflectance spectra, but the results can be highly dependent on the multivariate calibration technique and samples used in the training dataset (Vohland *et al*., 2011). Kaplan and Milliken (2016) studied synthetic mixtures of a pure particulate organic compound mixed with different clay minerals in an attempt to assess several fundamental properties that may control organic absorption strength and shape in reflectance spectra. That study found that TOC was linearly correlated to the strength (band depth) of C-H vibration absorption bands (1.73, 2.31, and 3.42 μm) in spectra of montmorillonite, illite, and kaolinite mixed with Na-stearate ($C_{18}H_{35}NaO_2$), an aliphatic organic compound. Those

https://doi.org/10.1346/CCMN.2018.064092 Published online by Cambridge University Press

results also demonstrated that the albedo strongly controlled the slope of the band depth-TOC trend when the samples were artificially darkened with lampblack C. Converting from reflectance to single scattering albedo (SSA) using the Hapke (1993, 2008) radiative transfer model was found to reduce these albedo-related effects, which were similar to previous work that used reflectance data to estimate the water content of clays and other hydrous minerals (Milliken and Mustard, 2007).

The work presented here builds on the study of Kaplan and Milliken (2016) by using similar measurements and data analysis methods to examine the organics in bulk rock powders from a suite of natural sedimentary rocks. In particular, the present study focused on diagnostic features that arise due to vibrational absorption bands of organic compounds at NIR-MIR wavelengths, which is a range that also hosts diagnostic absorption bands for minerals commonly found in sedimentary environments (*e.g.*, clay minerals).

METHODS

Samples

The samples examined in this study were predominantly Proterozoic shales with independently measured mineralogy, TOC, and H/C values. A full list of samples used in this study is available, which includes the provenance, lithology, and organic properties (Table S1, deposited with the Editor-in-Chief and available at http://www.clays.org/JOURNAL/JournalDeposits.html). Further descriptions of these rocks and their kerogens can be found in the original references. Kerogen, described in this list, refers to insoluble organic matter of varied chemical composition that has been extracted from bulk rock powders and is the primary form of organic matter found in these samples.

Many of the rocks studied here are from drill cores in the McArthur Basin in Australia's Northern Territory (*i.e.* cores discussed in Abbott and Sweet, 2000; Johnston *et al*., 2008; Luo *et al*., 2016). In total, 33 McArthur Basin samples were analyzed. Within the basin, the McArthur, Nathan, and Roper Groups have been sampled using seven drill cores, five of which are included in the present study: Urapanga-3 (U3), Urapanga-4 (U4), Urapanga-5 (U5), Urapanga-6 (U6), and Golden Grove-1 (GG1). The Roper Group is known for its organic-rich shales and high organic content (Dutkiewicz *et al*., 2003). Kerogens from twelve of these bulk rock samples were extracted and provided to the present study by the laboratory of R. Summons (MIT). Kerogen was isolated using acid attack and although some pyrite remains, it does not affect the results of this study.

A second set of 15 sedimentary rock samples were described in Tosca *et al*. (2010). The samples are organic-rich shales, late Archaean to Mesoproterozoic in age, that have been moderately to intensely weathered. The clay mineralogy, TOC, and weathering history for these samples were described in Tosca *et al*. (2010), though TOC was re-measured at Brown University. A third set of bulk rock samples (n = 8) that were previously studied and characterized by the Precambrian Paleobiology Research Group (PPRG) was provided by J.W. Schopf (UCLA). Each of these samples has a corresponding kerogen sample that was isolated from it. The PPRG rocks are cherts and shales from a variety of locations that have H/C values that range from 0.02 to 0.8. An additional 30 PPRG kerogens were provided by the Summons Lab (MIT) and were characterized by Ferralis *et al.* (2016) and Schopf (1983).

Finally, an additional 27 reflectance spectra of oil shales and source rocks with higher TOC values were downloaded from the NASA Reflectance Experiment Laboratory (RELAB) spectral library and were examined for comparison with the low TOC content samples described above. Characteristics of the kerogen in these samples are not known, but the provenance, mineralogy, and organic chemistry of the toluene soluble portion of these rocks were provided in Hosterman *et al*. (1989).

Reflectance spectroscopy

Bulk rock samples (Table S1 in Supplemental Materials section) were crushed in an agate mortar and pestle and the powders were sieved to <45 μm using a mesh sieve. Although reflectance measurements are possible for intact rocks or unsieved particulate samples, this step minimizes spectral differences between samples due to particle size variations and increases the signal due to increased scattering. Samples that correspond to spectra of the oil shales and source rocks that were pulled from the RELAB database were not all crushed and sieved to <45 μm and instead represent unsorted materials.

Reflectance spectra of all rock powders and isolated kerogens were measured in the Department of Earth, Environmental, and Planetary Sciences at Brown University using a combination of spectrometers. The VIS-NIR measurements (0.5−2.5 μm) were collected using an Analytic Spectral Devices (ASD) FieldSpec 3 spectroradiometer (ASD Inc., Boulder, Colorado USA). A fiber optic light source was used to illuminate the samples at 30º from normal and the receiving fiber optic on the ASD instrument was positioned at 0º. Bare fibers for the light source and receiving fiber have a ~25º field of view (FOV) and were positioned a few cm above the sample to capture the entire area of the sample cup (~10 mm) in the FOV. The same samples were then measured at longer wavelengths (1.75−25 μm) using a Nicolet iS50 FTIR spectrometer (Thermo Scientific, Waltham Massachusetts, USA). The FTIR was equipped with a Praying Mantis diffuse reflectance attachment (Harrick Scientific, Pleasantville New York, USA) and a diffuse Au reflectance standard from Labsphere (North Sutton,

https://doi.org/10.1346/CCMN.2018.064092 Published online by Cambridge University Press

New Hampshire, USA) was used as a reference material. Each bulk rock spectrum was an average of 50 scans and each kerogen spectrum was an average of 100 scans or more.

For comparison with the bulk rock powders, one semi-polished thick section (7.1 × 5.2 mm) of a pyrite-bearing shale was mapped using a Bruker Lumos FTIR Microscope (Billerica, Massachusetts, USA). Spectra were collected for the 1.6–16 μm wavelength range with 825 pixels at a spatial resolution of ~200 × 200 μm per pixel.

Elemental analysis (C and H)

Subsets of the bulk rock powders were measured for organic C using a CE Instruments Model NC2100 Elemental Analyzer (CE Elantech, Inc., Lakewood New Jersey, USA) at Brown University. The reflectance spectra were first used to confirm that the samples were carbonate-free and, therefore, required no acid treatment prior to elemental measurement. Carbon (wt.%) values for ~8–10 mg aliquots of powder were reported here as total organic carbon (TOC).

Elemental abundances for the PPRG kerogens were obtained using traditional combustion elemental analyses as described by Schopf (1983), which provides a full description of the analysis method. Isolated organic matter is useful for understanding how organic composition affects spectral features in the absence of complicating factors due to a mineral matrix. The H/C ratio was chosen to represent organic composition as it is often used to characterize kerogen type and maturity and will change as a function of the aliphatic:aromatic ratio in the kerogen (Baskin, 1997). Twelve kerogen and bulk rock pairs with unknown H/C ratios prior to this study were analyzed at Huffman Hazen Laboratories (Golden, Colorado, USA) to obtain H and C values using an elemental analyzer. These are the U-3, U-4, and KEA samples that were provided by R. Summons and are listed first in the supplementary table (Table S1 in Supplemental Materials section). H/C is reported here as a ratio of atomic abundances and TOC is reported in weight percent.

Analysis of spectral data

All reflectance spectra were processed identically and the FTIR spectra were scaled and spliced to match the ASD spectral data at a wavelength of 1.8 μm. Scaling of the FTIR data was necessary to match the ASD data because the FTIR signal was maximized by slightly raising or lowering the sample dish, which affected the reflectance values by a scalar relative to the diffuse Au standard (which was at a fixed height). In order to calculate band depth values, the spectral continuum shape was first defined using an upper convex hull fit over a wavelength range defined by endpoints at 3.1 and 3.8 μm (these wavelengths are outside the C-H absorption features of interest). The reflectance values at these wavelengths were then divided by this spectral continuum and band depth values were calculated from the resulting continuum-removed spectrum.

Band depths were calculated at 3.27, 3.38, 3.42, 3.48, and 3.50 μm as well as the integrated area of all organic absorption bands from 3.1 to 3.8 μm (Figure 2). Other spectral parameters that included albedo (taken as the reflectance value at 1.7 μm, a wavelength with no absorption bands in the samples studied) and spectral slope between 0.45–0.9 μm were also examined. A principal components analysis was also performed on the full spectra and on the continuum-removed (3.1–3.8 μm) spectra, and focused on the first five principal components that accounted for the majority of the variance in the dataset. For the thick section map, band depths associated with Al-bearing clay minerals (*e.g.* illite, 2.21 μm) and H_2O in phyllosilicates (1.9 μm) were calculated from the continuum-removed spectra between 1.7 and 2.35 μm.

Spectral parameters (*i.e.* band depth, band area, spectral slope) were compared with TOC and H/C values to assess the importance of each of these

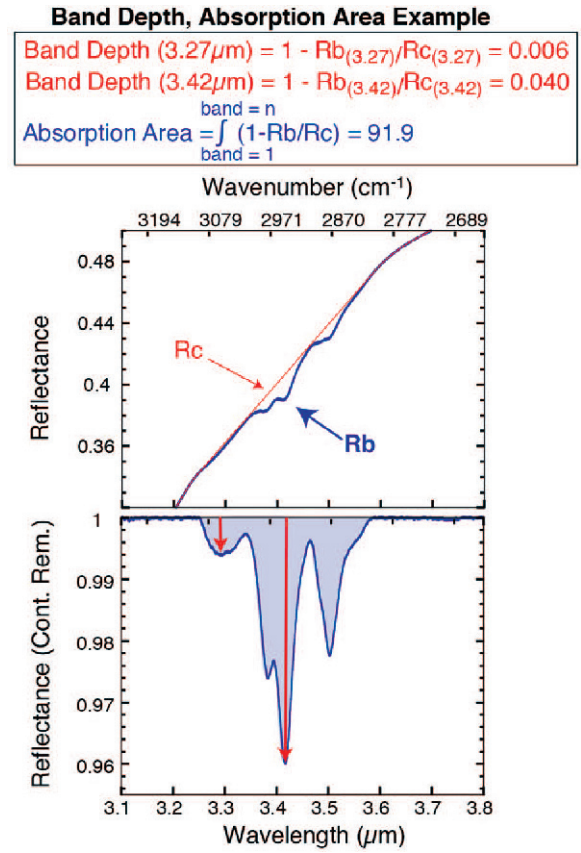

Figure 2. An example reflectance spectrum with an upper convex hull continuum fitted to it (top) and a continuum-removed spectrum with the continuum removed (bottom). The equations used for the major spectral parameters in this paper are given at the top.

https://doi.org/10.1346/CCMN.2018.064092 Published online by Cambridge University Press

variables and their quantitative influence on reflectance spectra. Relationships between these factors were assessed empirically and, when possible, using statistical methods. Reflectance spectra were also converted to single scattering albedo (SSA) values using the radiative transfer model developed by Hapke (1993). This conversion reduced effects in the reflectance spectra that were caused by multiple scattering and the viewing geometry that may give rise to changes in absorption strength that are not related to the abundance of an absorbing component. The spectral analyses described above were conducted for all SSA spectra, but no significant differences were found between reflectance and SSA results; therefore, the SSA results are not discussed here.

Bulk rock samples were removed from the spectral dataset if they displayed evidence of carbonates near 3.4 μm instead of the aliphatic organic 'triplet' absorption bands. The issues that surround the spectral interpretation of organics in the presence of carbonates were considered and are discussed in the discussion section, but the analyses were performed on carbonate-free or carbonate-poor bulk rock spectra.

RESULTS

Kerogen and bulk rock spectra

Reflectance spectra of the kerogen samples (Figure 1) typically exhibited vibrational absorption bands due to OH, alkyl C-H, C=O, C=C aromatic and polyaromatic rings, and aromatic C-H. Of these absorption bands, only the alkyl C-H stretching commonly appeared in spectra of the bulk rock powders, where it occurred as a 'triplet' absorption feature near 3.4 μm. Though superimposed on broader H_2O absorption bands in the ~2.65–4 μm wavelength region, the C-H absorption band at ~3.4 μm occurs at a position that has few overlapping mineral absorption bands in comparison to the other spectral features listed above, though carbonate is a notable exception. Spectra of kerogens with low H/C values (more aromatic, greater maturity) had weaker absorption bands in this wavelength region in comparison to those bands for samples with higher H/C values (more aliphatic, immature). This was as expected because the aliphatic bonding environment gives rise to the strongest spectral features in this wavelength region (Figure 1). In general, as H/C decreased, the absorption bands weakened and the spectrum became flatter and nearly featureless for samples with the lowest H/C values.

Spectra of bulk rock powders exhibited similar absorption bands as the kerogen with additional absorption bands in the VIS-NIR (0.35–2.5 μm) range due to minerals, which were primarily metal-OH vibrations associated with clay minerals and electronic absorption bands due to $Fe^{2+/3+}$-bearing phases (Figure 1). The OH/H_2O absorption bands from ~2.65 to 4 μm were stronger than in the corresponding kerogen spectra, whereas the C-H absorption bands near 3.4 μm were weaker. This was consistent with the organic signal being 'diluted' when in a mineral matrix. Unlike the kerogens, which are purely organic, both H/C and total organic carbon (TOC, *i.e.* organic abundance) were expected to affect properties of the ~3.4 μm absorption band in bulk rock powders.

Relationships between H/C, TOC, and spectral parameters

Measurements of TOC, H/C, and spectral attributes for these samples allowed the exploration of empirical relationships between these parameters as well as the lower limits of H/C and TOC values at which absorption bands can no longer be discerned in the reflectance spectra. Independently measured H/C values were compared to three spectral parameters (absorption area, band depth, and a ratio of the two band depths) (Figure 3). A comparison of the H/C values and absorption areas for kerogens (Figure 3a) revealed that when H/C was <0.2, the absorption bands near ~3.4 μm were absent or negligible. For some spectra, absorption bands were absent or were indistinguishable from background noise at these low H/C values. For other spectra, the absorption bands were very weak with absorption areas <10. Absorption area increased linearly with H/C for $0.2 < H/C < 1$. Albedo, water content of the kerogen, and particle size can affect the strength of C-H absorption bands (*e.g.* Kaplan and Milliken, 2016) and may influence the scatter. Overall, spectra of the kerogen samples suggested a lower detection limit for H/C ~0.2 and below this limit the detection of organics at these wavelengths in reflectance spectra will be difficult, regardless of the TOC.

Similar analyses for the bulk rock powders were carried out (Figure 3). For these samples, the absorption area was commonly weaker than in the kerogen spectra. As with the kerogens, absorption bands were weak or absent for H/C <0.2, but in the bulk rock powders this trend continued until H/C ~0.6. Above H/C ~0.6, clearly detectable C-H absorption bands were observed in this wavelength region. Note, however, that the bulk rock samples with weak absorption bands and H/C values between 0.2 and 0.6 also had TOC values <1 wt.% (*i.e.* the concentration of organic matter in the sample as a whole was low). For samples with measured H/C values (*e.g.* those shown in Figure 3), the TOC values ranged from 0.25–8.68 wt.%. Another 41 samples with unknown H/C ratios had a TOC range of 0.13 of 3.45 wt.% (Table S1 in Supplemental Materials section).

Band depth values at 3.42 and 3.27 μm were plotted against H/C for both kerogen and bulk rocks (Figure 3b). Band depth at 3.42 μm, which is an aliphatic CH_2 absorption band and the strongest band in this wavelength region, had a similar relationship to H/C as absorption area for both the kerogen and bulk rock

https://doi.org/10.1346/CCMN.2018.064092 Published online by Cambridge University Press

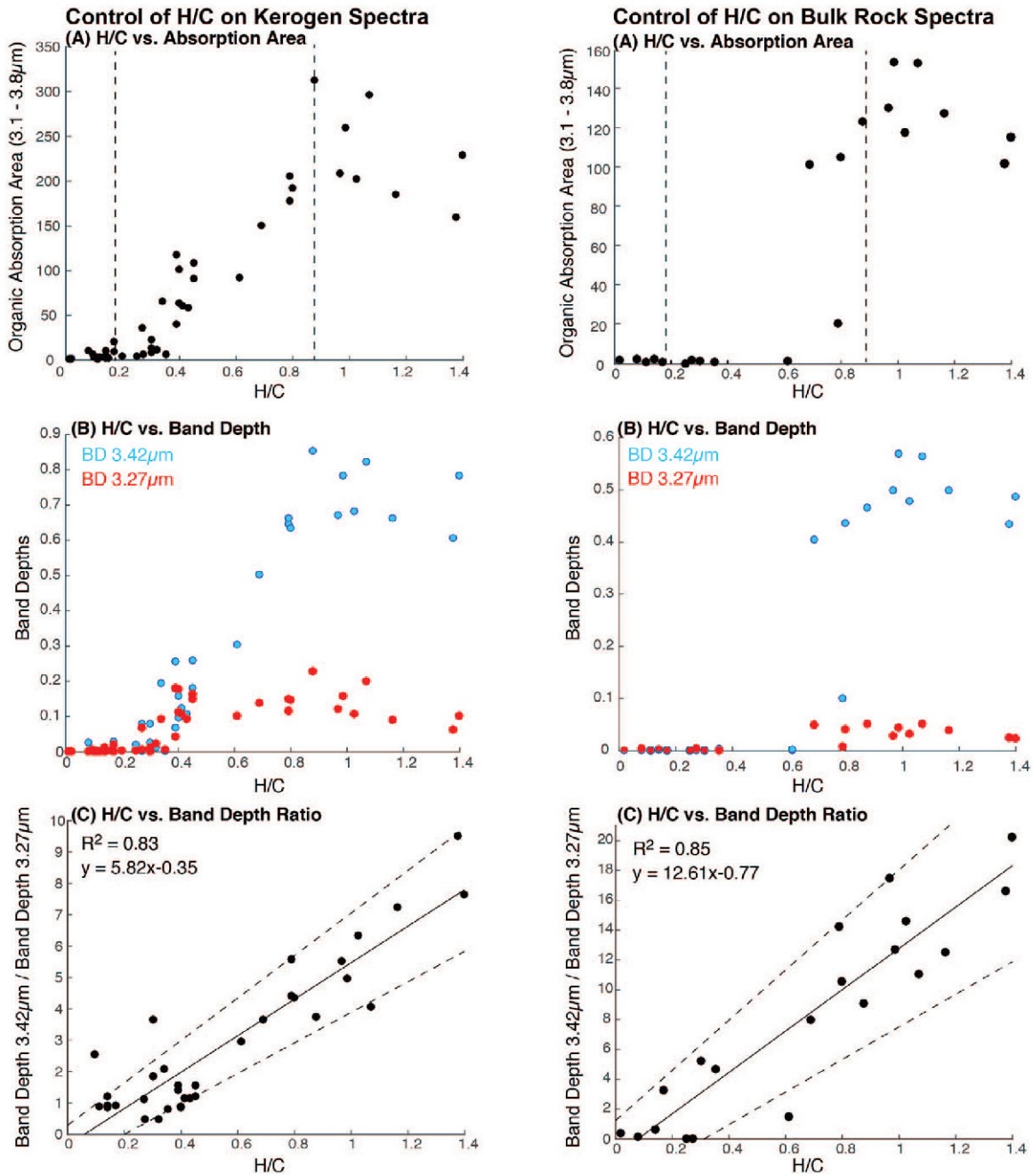

Figure 3. These plots show the relationships between H/C and absorption area, band depths, and band depth ratios. The plots on the left are isolated kerogens, while the plots on the right are bulk rock samples with known H/C values. (a) The absorption area in general increased with increased H/C value and the dotted lines at H/C = 0.2 and 1 reflect breaks in this trend. (b) The band depths at 3.42 and 3.27 μm are for aliphatic and aromatic C-H absorption bands, respectively; The aliphatic absorption band followed a similar trend as absorption area, while the aromatic absorption band increased more strongly initially and then flattens and remained weaker at higher H/C values. (c) A linear relationship was observed between H/C values and the aliphatic to aromatic absorption band depth ratios and a least squares regression line with 95% confidence intervals (dotted lines) are included.

samples. Band depth at 3.27 μm, which is an aromatic C-H absorption band, was much weaker at most H/C values. In the kerogens, band depth values at 3.27 μm rose sharply for 0.2 < H/C < 0.4 and then leveled off or diminished at higher H/C values. In bulk rocks, band depth at 3.27 μm was consistently weak at all H/C values >0.6. The ratio of band depth at 3.42 μm (aliphatic) to band depth at 3.27 μm (aromatic) was strongly correlated with H/C for both kerogen and bulk rock samples (Figure 3c).

https://doi.org/10.1346/CCMN.2018.064092 Published online by Cambridge University Press

A comparison among albedo, organic absorption area, and VIS-NIR slope values for the kerogen/bulk rock sample pairs was performed (Figure 4). These trends suggest that all three spectral properties observed in the kerogen spectra were strongly correlated with the VIS-NIR slope and the absorption area in the corresponding bulk rock spectra. In contrast, the albedo of the bulk rocks appeared to be unrelated to the kerogen properties and likely reflected the mineralogy rather than the organic matter in the rock. For these samples at least, VIS-NIR slope values from the bulk rock spectra can be used to estimate absorption area and, from that, to estimate the H/C-TOC properties of the organics.

Principal components analysis (PCA) results

PCA as it was applied to the continuum-removed spectra of the bulk rock samples showed that the first two principal components (PCA 1, PCA 2) explain over 98% of the variance in the data. These two components, when plotted against each other for each bulk rock powder, exhibited a linear trend that can be used to separate different groups within the sample set (Figure 5). The oil shales/source rocks were included in this analysis because it was based solely on the spectral characteristics, whereas these samples were not included in the previous analyses because the properties of the kerogen fraction were unknown. Despite this difference, or perhaps because of it, the oil shales/source rocks occupied a unique PCA-space. Other sample groups were also shown to occupy distinct portions of the plot. These sample groups can be divided by using the H/C values. The same plot with points colored by the H/C values confirmed that H/C plays a major role in determining where the samples fall on the trend. Samples with the lowest H/C values exhibited larger values in both PCA 1 and PCA 2 (see inset, Figure 5). In contrast, samples with higher H/C values generally exhibited smaller PCA values, though samples with some of the highest H/C values fell along the middle of the trendline.

In addition to the H/C values, the data demonstrated that TOC values also affected the PCA results (Figure 5). The highest and lowest TOC values fell at the extremes of the linear trend and samples in the middle of the plot

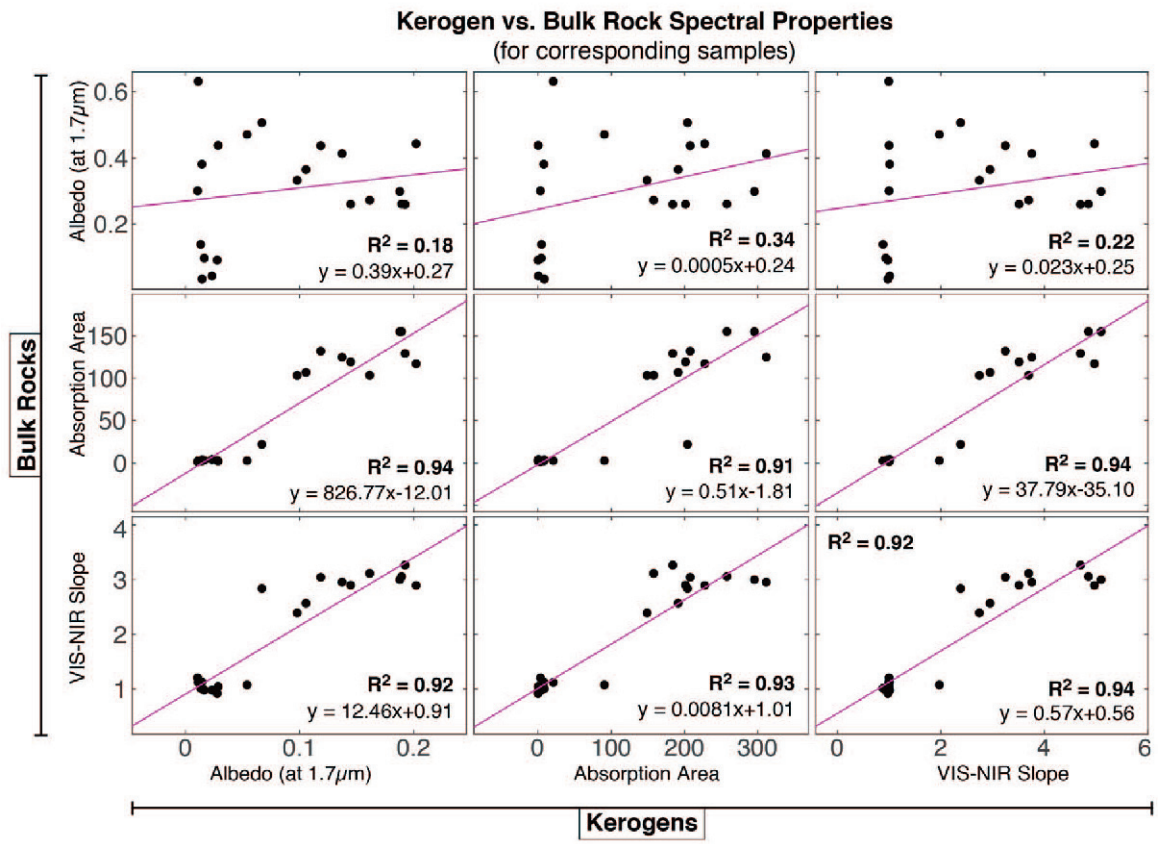

Figure 4. Correlation matrix for the bulk rock and extracted kerogen samples, where each point reflects the parameter (albedo, absorption area, VIS-NIR slope) values of the bulk rock and the extracted kerogen samples. The albedo was measured at 1.7 μm, the organic absorption area was determined, and the VIS-NIR slope was calculated between 0.9 and 0.44 μm. For example, the top left plot shows the relationship between the bulk rock and kerogen sample albedo values, but in this case the bulk rock and kerogen sample albedo values were not strongly correlated.

https://doi.org/10.1346/CCMN.2018.064092 Published online by Cambridge University Press

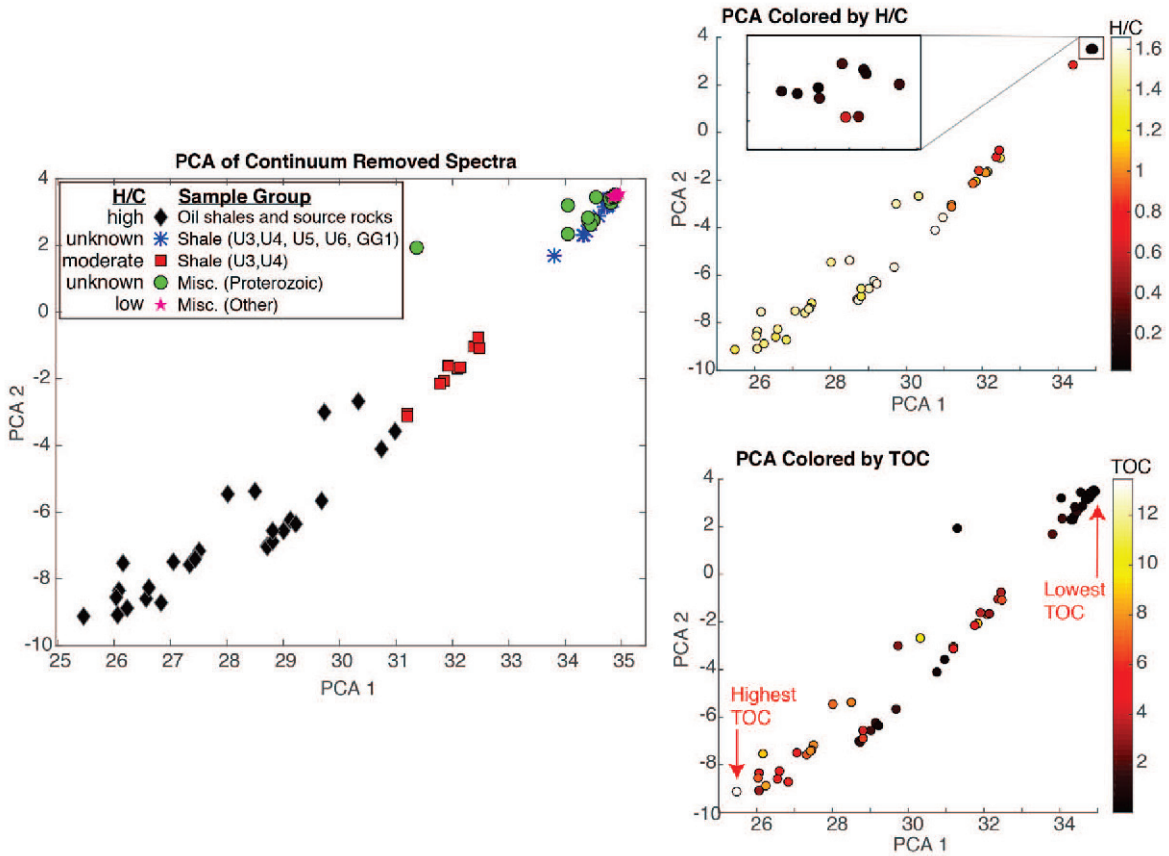

Figure 5. The first two principal components (PCA 1, PCA 2) were plotted for bulk sedimentary rocks and for 27 oil shales and source rocks. In PCA space, the samples grouped together with samples from similar groups (*e.g.* shales with moderate H/C, oil shales with high H/C). Modified versions of the left plot are shown on the right with points colored according to the H/C and TOC values. An apparent relationship was observed between the principal component values (PCA 1, PCA 2) and the rock H/C and TOC values.

with high H/C values also had low TOC values, which may explain why the samples plotted in this part of the parameter space. To confirm this finding, a linear least squares regression was performed and revealed that both H/C and TOC values were statistically significant predictors of the first principal component ($p = 6.6e^{-13}$ and $p = 2.0e^{-3}$ for H/C and TOC) and the second principal component ($p = 2.6e^{-15}$ and $p = 0.002$ for H/C and TOC).

DISCUSSION

Lower limits of detection and quantification

The results show that the presence and strength of organic absorption bands in the 3.1−3.8 μm region were clearly tied to the H/C values of the pure organic matter (kerogen). Spectra of bulk rocks, however, were not only affected by the composition of the organics but also by the abundance of that organic component. Absorption areas for the bulk rocks can also be plotted in terms of both H/C and TOC (Figure 6) values. The 21 bulk rock samples with known H/C and TOC values spanned a range in H/C from 0 to 1.4 and in TOC from 0 to 9 wt.%. As demonstrated above (Figure 6), spectra for bulk rocks with H/C < 0.2 had weak or absent organic absorption bands, even if the TOC value was high. Samples with H/C > 0.2 and reflectance spectra without organic absorption bands also contained ⩽1 wt.% TOC. A very conservative TOC detection limit of 1 wt.% was proposed by Kaplan and Milliken (2016) based on synthetic clay-organic mixtures and is marked with the dotted line in Figure 6. Carbonaceous chondrite meteorites have up to 4 wt.% organic C and H/C values between 0.2 and 0.8, which places these samples above the detection limits and makes it likely that organic analysis with reflectance spectroscopy will be beneficial.

In all likelihood, a uniform TOC limit is not appropriate for all organic-bearing samples and many samples with TOC values <1 wt.% (listed in Table S1 in Supplemental Materials section) had reflectance spectra with organic absorption bands, but without measured H/C values. The TOC threshold may be lower with greater H/C values (as indicated by the red (light gray, grayscale) curved dotted line in Figure 6), though some minimum TOC value without observed absorption bands was expected. Although the exact lower TOC

https://doi.org/10.1346/CCMN.2018.064092 Published online by Cambridge University Press

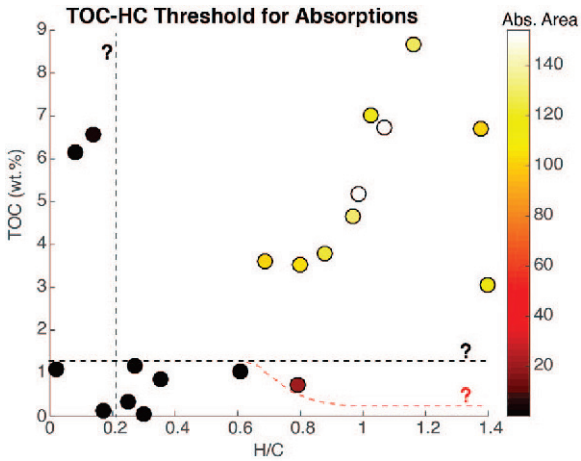

Figure 6. Bulk rock samples were plotted according to the TOC and H/C values and were colored (white to gray in grayscale) according to absorption area values. Only the samples that fell in a specific TOC-H/C space had absorption bands and are identified by the colored circles (*i.e.* the black circles indicate no absorption band). The straight black, dotted lines indicate the approximate lower detection limits for H/C and TOC. The H/C detection limit was ~0.2 and was supported by the kerogen spectral results. The TOC detection limit was ~1 wt.% and decreased as the H/C value increased above 0.6 (red curved dotted line, gray in grayscale).

detection limit was not defined with the limited sample suite examined here, evidence in the sample collection suggests that it could be ~0.1%. For instance, drill core sample 22 from the McArthur Basin had TOC values that ranged from 0.13 to 0.62 wt.%, yet spectra for all of these bulk rock powders had clear organic absorption bands. Based on these results using reflectance spectroscopy, an important although variable parameter space for H/C and TOC values likely exists, but defining a lower organic matter detection limit for bulk rocks (or at least shales) will not be possible at these wavelengths. Further studies on samples that span a wider TOC and H/C range than discussed here, particularly samples with high H/C and low TOC values, are warranted to better establish independent detection limits for H/C and TOC. Establishing the probable lower detection limits for organics is especially important to fully realize reflectance spectroscopy as a method in planetary applications where direct sampling is not always possible. Ongoing and planned missions will immediately benefit from additional constraints on the collected data. For instance, recent results from the Dawn mission to Ceres revealed a strong aliphatic spectral signature near the Ernutet crater (De Sanctis *et al*., 2017), but the estimated TOC and H/C values are currently poorly understood.

From the data presented here, the best constraints on detection limits come from the kerogen spectra. These spectra showed weak or absent absorption bands for H/C values of <~0.2. This result was physically plausible because the decrease in H/C values occurred as the kerogen became more aromatic in nature and C-H bonds were replaced with C=C bonds. As the C-H bonds disappeared, so did the entire absorption complex between 3.1 and 3.8 μm (*e.g.*, Figure 1). Similarly, an increase in the aliphatic C-H to aromatic C-H ratio with increased H/C values would be reasonable, as demonstrated by the 3.42 to 3.27 μm band ratio. When absorption area or band depth was used for samples in the present study, these parameters became non-unique predictors for H/C values >1. No indication of absorption band saturation was observed in the spectral data, thus one explanation for this trend is that the number of CH_2 and/or CH_3 groups did not increase directly for H/C values >1.

These lower detection limits were dependent on the signal-to-noise ratio of the instrument used for spectral acquisition. Many of the organic absorption bands treated in the present study determined to be 'below' detection limits were in fact observable in the FTIR data, but were very weak (*i.e.* absorption area <10 or band depth <0.01). While the detection of these very weak absorption bands was possible in a laboratory setting, observing similarly weak signatures would be unlikely in data acquired in a less controlled scenario. Lower signal-to-noise ratios for field and orbital measurements are likely to further increase the HC-TOC thresholds for detection of organic matter in these applications.

The number of samples with known H/C and TOC values is small (n = 21), which makes statistical analysis of the relative contributions of H/C and TOC values to band depth and PCA spectral parameters difficult. With this caveat, a linear regression was carried out to assess the influence of normalized H/C and TOC values on band depth at 3.42 μm, PCA 1, and PCA 2. From this analysis, the strongest spectral influence was from H/C as it had a larger regression coefficient and a lower p-value for each case (Table 1). These coefficients were needed to solve for both H/C and TOC values from these spectral parameters, but more testing is necessary to prove their efficacy for a wider range of samples. If either the H/C or TOC value is known and is relatively homogeneous within the measurement spot size or between measurements, however, the absorption strength at ~3.4 μm in reflectance spectra can be a powerful predictor of the other attribute.

Important considerations for organic detection and quantification

The above results pertain to the clay-rich shales discussed in the present paper. Carbonate reflectance spectra exhibit absorption features that overlap with C-H vibrations in the mid-infrared and can complicate these assumptions. Washburn *et al*. (2015) successfully predicted calcite, dolomite, and TOC values using partial least squares regression (PLSR) applied to attenuated total reflectance (ATR) measurements. In that work, the authors studied oil shales from the Green River Fm.,

https://doi.org/10.1346/CCMN.2018.064092 Published online by Cambridge University Press

Table 1. Regression coefficients, error estimates, and p-values for normalized H/C and TOC regressed against band depth (3.42 μm), PCA 1, and PCA 2. The normalized H/C values have larger coefficient (estimate) values and lower p-values for both PCA 1 and PCA 2.

y Term	Parameter (x)	Estimate	t Statistic	p-Value
Band depth (3.42 μm)	norm. H/C	0.27	12.97	$3.84 \times ^{-17}$
	norm. TOC	0.05	2.65	$1.11 \times ^{-02}$
PCA 1	norm. H/C	−2.31	−9.78	$6.62 \times ^{-13}$
	norm. TOC	−0.92	−4.03	$2.00 \times ^{-04}$
PCA 2	norm. H/C	−3.61	−11.54	$2.62 \times ^{-15}$
	norm. TOC	−0.95	−3.16	$2.78 \times ^{-03}$

which had spectra with overlapping organic and carbonate absorption bands near 3.4 μm. For rocks with lower TOC values and/or more mature organics, even small amounts of carbonate can overwhelm the organic absorption bands and prevent detection using reflectance spectra (in the absence of *a priori* knowledge that organics are present). Ongoing work will focus on adding carbonate abundance to the H/C-TOC parameter space (Figure 6) to add further constraints to organic detection, which is an important aspect given that carbonate minerals are common in terrestrial sedimentary basins and are found in organic-bearing C chondrite meteorites. Quantifying and subsequently removing carbonates from the spectrum may be possible as part of the continuum removal process, as demonstrated by Herron *et al*. (2014) and Craddock *et al*. (2017).

Other rock properties are likely to have a lesser effect on the detection of organic absorption bands in the 3 to 4 μm wavelength region, but should still be considered for future applications. Kaplan and Milliken (2016) found that albedo was strongly correlated to organic band depth at 3.42 μm, but that conversion from reflectance to single scattering albedo reduced this issue. A similar relationship between sample albedo and water content (based on strength of H_2O absorption bands at ~3 μm) was observed by Milliken and Mustard (2007), who also demonstrated that conversion to SSA greatly reduced non-linear absorption effects in dark samples. In the present work, albedo does not appear to play a major role and albedo in the bulk rock samples appeared to be controlled by mineralogy rather than organic content (Figure 4). Mineralogy of the bulk rock samples was diverse and did not seem to influence organic absorption bands near 3.4 μm. The exception was carbonate and, as a result, the present study was carried out on bulk rocks that were spectrally free of carbonates at 3.4 μm. The observation that different subsets of the sample suite could be identified using principal components analysis likely did not reflect similarities in mineralogy because the PCA was done on continuum-removed spectra over a limited wavelength range that was outside of most mineral absorption bands.

Another issue to be considered is sample heterogeneity, which may lead to compositional differences between sample aliquots that are used for reflectance measurements and those used for measuring TOC and elemental abundances. Within a given bulk powder, some difference may exist in spectral features that depend on sample particle size and illuminated area (see discussion in Kaplan and Milliken, 2016). Variations related to sample heterogeneity were emphasized in data from the thick section imaging (Figures 7−8), which are discussed below. Each measured spectrum exhibited slightly different properties based on spatial position.

Spectral mapping

A primary goal of the present study was to provide a foundation for the quantitative application of reflectance spectroscopy to mapping variations in organic matter across hand samples, outcrops, and planetary surfaces. As a case study for an intact rock sample, reflectance spectra for a portion of a thick section (~7 × 5 mm) of a pyrite-bearing shale from the McArthur Basin (U-4 64.7m) were measured using an FTIR microscope. The H/C value of the kerogen in this sample was unknown, but the bulk sample was measured and had a TOC of 0.86 wt.%. The spectra were acquired in a grid and resulted in a total of 825 spectra to produce a 'map' of the thick section that showed a range of organic absorption strengths along with evidence of Al-bearing clay minerals (illite) and minor carbonate (Figure 7). Band depth values were calculated for each spectrum using the procedures discussed above, with the addition of band depth calculations at 1.9 μm for H_2O and at 2.21 μm for Al-OH (proxy for illite/muscovite content). The spectra were also transformed into the same PCA space as the bulk rock powders described above.

The PCA 1 and PCA 2 values for the thick section grouped along the same region as the bulk rock powders and, in fact, clustered around the powdered sample of U-4 64.7m and other powders from the same drill core (Figure 7). Each powder was a homogenized version of the original rock and plotted as a single point in PCA-space, but the chip showed the true heterogeneity of a

https://doi.org/10.1346/CCMN.2018.064092 Published online by Cambridge University Press

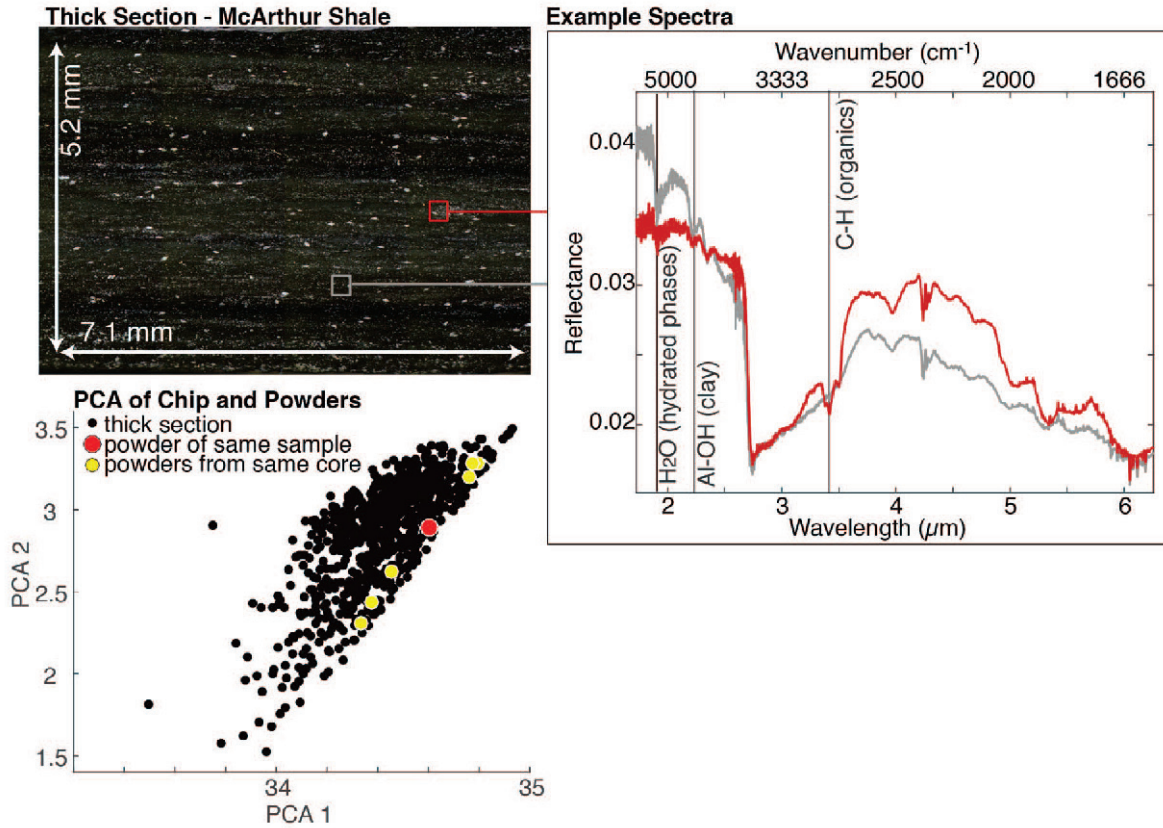

Figure 7. An optical microscope image of the McArthur shale (U-4 64.7m) thick section, which was mapped using 825 (~200 × 200 μm) pixels. The spectra on the right are from different parts of the thick section. These spectra show a range in organic absorption strength as well as absorption bands due to Al-clay minerals (illite/muscovite). The principal components (PCA 1, PCA 2) of the thick section were plotted to compare the PCA 1 and PCA 2 values for the thick section, bulk powder, and nearby samples from the same drill core.

single sample and revealed the possibility to reconstruct spatial variations in H/C and TOC.

Within the spectral map were coherent regions of high and low aliphatic organic content that corresponded to visible layers in the sample. Organic (3.42 μm), Al-clay (illite/muscovite), and H_2O distributions were compared spatially (Figure 8). Laminations with higher clay and water contents exhibited weaker organic bands, which was not intuitive given the known associations between organics and clay minerals (*e.g.* Keil and Mayer, 2014). In addition to band depths, the first and second principal components were displayed spatially. The PCA 1 value revealed no obvious spatial correlation, but PCA 2 was highly spatially correlated with the 3.42 μm band depth. The PCA 1 and PCA 2 values were both used to create an RGB image (where the PCA values were normalized and the third band was set to 1) (Figure 8, bottom right). The position of these PCA values on a PCA 1 *vs*. PCA 2 plot was recorded (Figure 8, bottom left), making possible the determination of how the values relate to the other samples in the study. In general, the darker purple (dark gray in grayscale) regions corresponded to higher TOC-H/C values than the lighter purple (light gray in grayscale) regions based on bulk sample analysis using PCA 1 and PCA 2 (Figure 5).

Band depth at 3.42 μm and band depth ratios (not shown in figure) suggested that the H/C values fall between 0.2 and 0.6. The position of points on the PCA scatter plot predicted TOC values <2 wt.%. If the goal were to find most of the organic rich portions of the sample for further analysis, the darker layers in the thick section would be the primary targets. Darker lamina-

Figure 8 (*facing page*). The McArthur shale thick section shown in Figure 7 is shown using maps for the different spectral parameters: band depth at 1.9 μm, band depth at 2.21 μm, band depth at 3.42 μm, the first principal component PCA 1, and the second principal component PCA 2. The regions of greater clay and organic contents are revealed in the maps and correlate to dark layers in the visible image (upper left). An RGB image (bottom right) of the thick section was prepared using PCA 1 and PCA 2 values. The circles in the PCA 1 *vs*. PCA 2 plot (bottom left) mark the thick section and core sample powder PCA 1 and PCA 2 values.

https://doi.org/10.1346/CCMN.2018.064092 Published online by Cambridge University Press

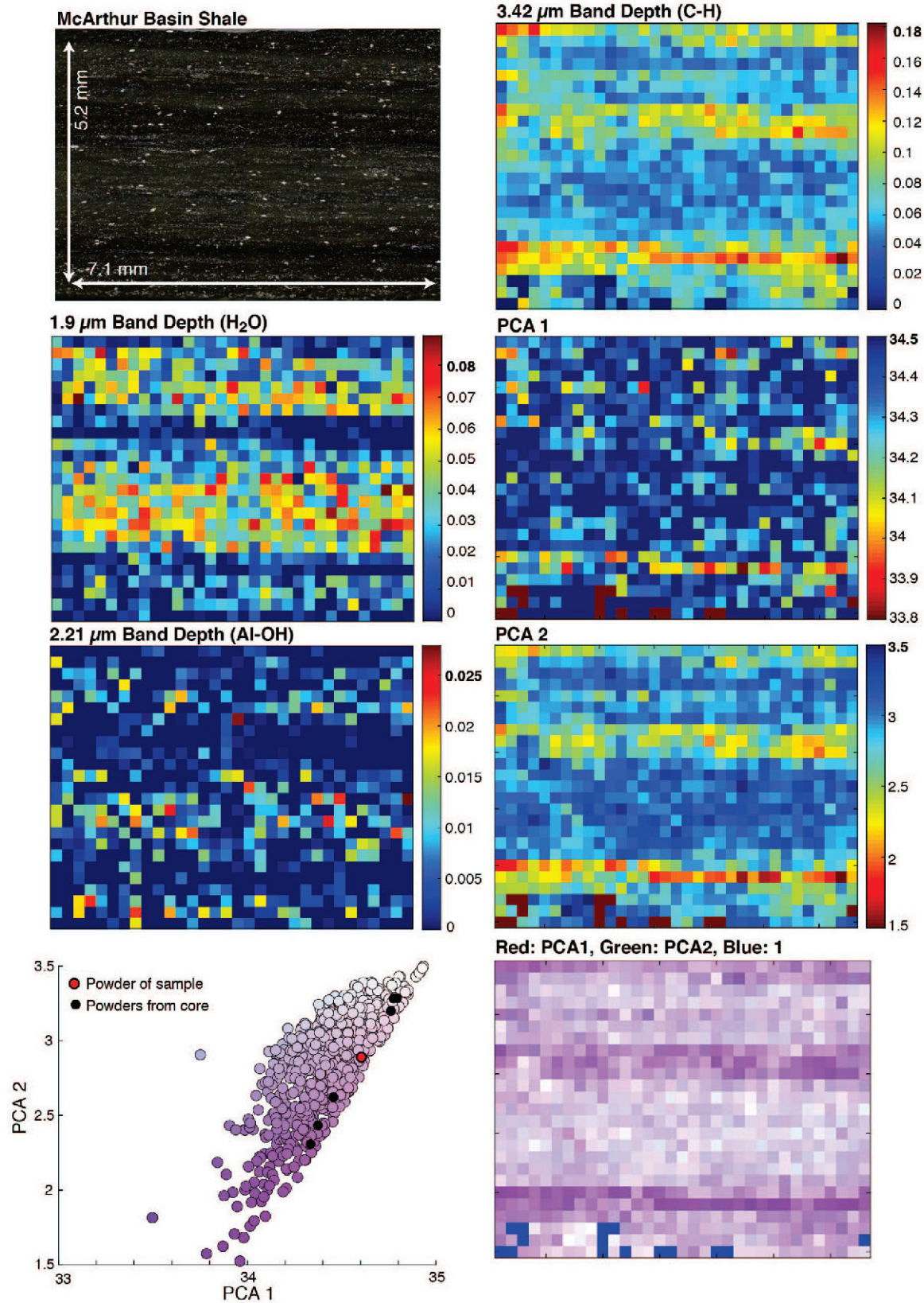

https://doi.org/10.1346/CCMN.2018.064092 Published online by Cambridge University Press

tions/zones that are enriched in organic material are not uncommon in terrestrial mudrocks, but the same is not necessarily true for planetary surfaces or materials. Many carbonaceous chondrite meteorites, for instance, are dark but lack organic compounds. The same is presumably true for certain low-albedo asteroids. In these cases, visible albedo is a poor estimator of organic content and highlights the utility of near-IR spectral reflectance data that can identify diagnostic C-H absorption bands. Issues remain when transitioning from point powder measurements to these spectral maps of thick sections. The particle size distribution was unknown and less scattering was returned from the thick section and led to a reduced albedo. Significant albedo differences between the sedimentary layers may also influence the compositions determined from spectra. Despite these caveats, this case study demonstrated that the spectral parameters discussed in the present paper can be applied to a spectral image and used to map regions of higher and lower TOC-H/C, as well as make general estimates of TOC and H/C values.

CONCLUSIONS

Using NIR-MIR reflectance spectra, a number of spectral parameters were found to correlate to organic abundance (TOC) and composition (H/C) in ancient shales and the isolated kerogen samples. Absorption areas, individual band depths (3.42 μm and 3.27 μm), and organic band depth ratios (3.42 μm / 3.27 μm) all increased with increased H/C values for both kerogens and bulk rock powders. Absorption bands were not clearly observed in spectra of isolated kerogen samples with H/C <0.2 and placed a limit on the detection of mature, aromatic-dominated organics using this technique. In addition to H/C values, TOC also strongly affected organic absorption bands in reflectance spectra of bulk rock powders. The lower TOC detection limit was predicted to vary based on the H/C value of the kerogen. When the H/C was low, the TOC detection limits were estimated to be 1 wt.%, but this limit was expected to decrease to $\leqslant$0.1 wt.% in samples with higher H/C values. Further constraint of these limits is critical to properly detect and identify organic components in geologic materials using reflectance spectroscopy in the laboratory, field, or remotely sensed applications. As an example, an observed lack of organic absorption bands in the NIR-MIR reflectance spectra of C-type asteroids that will soon be acquired by the Hayabusa2/MASCOT and OSIRIS-REx missions may reflect attributes of organic composition (low H/C values) rather than an absence of organic compounds on these bodies.

In addition to spectral parameters, principal component decomposition values were statistically related to TOC and H/C for the shales and previously measured source rocks whose spectra were examined in the present study. An example of applying principal components and spectral parameters to a thick section of an organic-bearing shale revealed that increased information can be gained when spectra are resolved at small spatial scales (as opposed to point measurements of bulk rocks). Such data can be used to assess qualitative differences in organic content/composition across a sample, including estimated TOC and H/C ranges, and in principle these methods can be applied to larger spatial scales for reflectance data acquired in field and orbital settings. Obtaining quantitative estimates of H/C and TOC based solely on reflectance spectra is nontrivial, however, if neither property is known *a priori*, because both will influence C-H absorption strength in the spectra of bulk rocks. At a minimum, a combination of parameters is needed to provide this information under these conditions.

ACKNOWLEDGMENTS

The authors acknowledge the NASA Astrobiology Institute (CAN 6: Foundations of Complex Life) for funding, and Bill Schopf, Andrew Knoll, and Roger Summons for providing samples. The authors also thank Editor-in-Chief Joseph Stucki, Associate Editor Michael Ploetze, Paul Craddock, and two anonymous reviewers for comments that helped to improve this manuscript. All data discussed in this paper are available through the corresponding author.

REFERENCES

Abbott, S.T. and Sweet, I.P. (2000) Tectonic control on third-order sequences in a siliciclastic ramp-style basin: An example from the Roper Superbasin (Mesoproterozoic), northern Australia. *Australian Journal of Earth Sciences*, **47**, 637–657.

Baskin, D.K. (1997) Atomic H/C ratio of kerogen as an estimate of thermal maturity and organic matter conversion. *AAPG bulletin*, **81**, 1437–1450.

Bibring, J.-P., Hamm, V., Pilorget, C., Vago, J.L., and the MicrOmega Team. (2017) The MicrOmega Investigation Onboard ExoMars. *Astrobiology*, **17**, 621–626.

Breen, C., Clegg, F., Herron, M.M., Hild, G.P., Hillier, S., Hughes, T.L., Jones, T.G.J., Matteson, A., and Yarwood, J. (2008) Bulk mineralogical characterisation of oilfield reservoir rocks and sandstones using diffuse reflectance infrared Fourier transform spectroscopy and partial least squares analysis. *Journal of Petroleum Science and Engineering*, **60**, 1–17.

Calderón, F., Haddix, M., Conant, R., Magrini-Bair, K., and Paul, E. (2013) Diffuse-reflectance Fourier-transform mid-infrared spectroscopy as a method of characterizing changes in soil organic matter. *Soil Science Society of America Journal*, **77**, 1591–1600.

Capaccioni, F., Coradini, A., Filacchione, G., Erard, S., Arnold, G., Drossart, P., De Sanctis, M.C., Bockelee-Morvan, D., Capria, M.T., Tosi, F., Leyrat, C., Schmitt, B., Quirico, E., Cerroni, P., Mennella, V., Raponi, A., Ciarniello, M., McCord, T., Moroz, L., Palomba, E., Ammannito, E., Barucci, M.A., Bellucci, G., Benkhoff, J., Bibring, J.P., Blanco, A., Blecka, M., Carlson, R., Carsenty, U., Colangeli, L., Combes, M., Combi, M., Crovisier, J., Encrenaz, T., Federico, C., Fink, U., Fonti, S., Ip, W.H., Irwin, P., Jaumann, R., Kuehrt, E., Langevin, Y., Magni, G., Mottola, S., Orofino, V., Palumbo, P., Piccioni, G., Schade, U., Taylor, F., Tiphene, D., Tozzi, G.P., Beck, P., Biver, N.,

https://doi.org/10.1346/CCMN.2018.064092 Published online by Cambridge University Press

Bonal, L., Combe, J.-P., Despan, D., Flamini, E., Fornasier, S., Frigeri, A., Grassi, D., Gudipati, M., Longobardo, A., Markus, K., Merlin, F., Orosei, R., Rinaldi, G., Stephan, K., Cartacci, M., Cicchetti, A., Giuppi, S., Hello, Y., Henry, F., Jacquinod, S., Noschese, R., Peter, G., Politi, R., Reess, J.M., and Semery, A. (2015) The organic-rich surface of comet 67P/Churyumov-Gerasimenko as seen by Virtis/Rosetta. *Science*, **347**, aaa0628.

Chang, C.-W., Laird, D.A., Mausbach, M.J., and Hurburgh, C.R. (2001) Near-infrared reflectance spectroscopy–principal components regression analyses of soil properties. *Soil Science Society of America Journal*, **65**, 480.

Chen, Y., Furmann, A., Mastalerz, M., and Schimmelmann, A. (2014) Quantitative analysis of shales by KBr-FTIR and micro-FTIR. *Fuel*, **116**, 538–549.

Christy, A.A., Hopland, A.L., Barth, T., and Kvalheim, O.M. (1989) Quantitative determination of thermal maturity in sedimentary organic matter by diffuse reflectance infrared spectroscopy of asphaltenes. *Organic Geochemistry*, **14**, 77–81.

Clark, R.N. and Roush, T.L. (1984) Reflectance spectroscopy: Quantitative analysis techniques for remote sensing applications. *Journal of Geophysical Research*, **89**, 6329–6340.

Clark, R.N., Curchin, J.M., Hoefen, T.M., and Swayze, G.A. (2009) Reflectance spectroscopy of organic compounds: 1. Alkanes. *Journal of Geophysical Research*, **114**, E03001, https: //doi.org/10.1029/2008JE003150.

Clark, R.N., Curchin, J.M., Barnes, J.W., Jaumann, R., Soderblom, L., Cruikshank, D.P., Brown, R.H., Rodriguez, S., Lunine, J., Stephan, K., Hoefen, T.M., Le Mouélic, S., Sotin, C., Baines, K.H., Buratti, B.J., and Nicholson, P.D. (2010) Detection and mapping of hydrocarbon deposits on Titan. *Journal of Geophysical Research*, **115**, E10005, doi: 10.1029/2009/2009JE003369.

Cloutis, E., Gaffey, M.J., and Moslow, T.F. (1994) Spectral Reflectance Properties of Carbon-Bearing Materials. *Icarus*, **107**, 276–287.

Coradine, A., Capaccioni, F., Drossart, P., Semery, A., Arnold, G., Schade, U., Angrilli, F., Barucci, M.., Bellucci, G., Bianchini, G., Bibring, J.., Blanco, A., Blecka, M., Bockelee-Morvan, D., Bonsignori, R., Bouye, M., Bussoletti, E., Capria, M.., Carlson, R., Carsenty, U., Cerroni, P., Colangeli, L., Combes, M., Combi, M., Crovisier, J., Dami, M., DeSanctis, M.., DiLellis, A.., Dotto, E., Encrenaz, T., Epifani, E., Erard, S., Espinasse, S., Fave, A., Federico, C., Fink, U., Fonti, S., Formisano, V., Hello, Y., Hirsch, H., Huntzinger, G., Knoll, R., Kouach, D., Ip, W.., Irwin, P., Kachlicki, J., Langevin, Y., Magni, G., McCord, T., Mennella, V., Michaelis, H., Mondello, G., Mottola, S., Neukum, G., Orofino, V., Orosei, R., Palumbo, P., Peter, G., Pforte, B., Piccioni, G., Reess, J.., Ress, E., Saggin, B., Schmitt, B., Stefanovitch, Stern, A., Taylor, F., Tiphene, D., and Tozzi, G. (1998) Virtis: An imaging spectrometer for the Rosetta mission. *Planetary and Space Science*, **46**, 1291–1304.

Coradini, A., Capaccioni, F., Drossart, P., Arnold, G., Ammannito, E., Angrilli, F., Barucci, A., Bellucci, G., Benkhoff, J., Bianchini, G., Bibring, J.P., Blecka, M., Bockelee-Morvan, D., Capria, M.T., Carlson, R., Carsenty, U., Cerroni, P., Colangeli, L., Combes, M., Combi, M., Crovisier, J., Desanctis, M.C., Encrenaz, E.T., Erard, S., Federico, C., Filacchione, G., Fink, U., Fonti, S., Formisano, V., Ip, W.H., Jaumann, R., Kuehrt, E., Langevin, Y., Magni, G., Mccord, T., Mennella, V., Mottola, S., Neukum, G., Palumbo, P., Piccioni, G., Rauer, H., Saggin, B., Schmitt, B., Tiphene, D., and Tozzi, G. (2007) Virtis: An Imaging Spectrometer for the Rosetta Mission. *Space Science Reviews*, **128**, 529–559.

Craddock, P.R., Prange, M., and Pomerantz, A.E. (2017) Kerogen thermal maturity and content of organic-rich mudrocks determined using stochastic linear regression models applied to diffuse reflectance IR Fourier transform spectroscopy (DRIFTS). *Organic Geochemistry*, **110**, 122–133.

Cruikshank, D.P., Dalle Ore, C.M., Clark, R.N., and Pendleton, Y.J. (2014) Aromatic and aliphatic organic materials on Iapetus: Analysis of Cassini VIMS data. *Icarus*, **233**, 306–315.

De Sanctis, M.C., Ammannito, E., McSween, H.Y., Raponi, A., Marchi, S., Capaccioni, F., Capria, M.T., Carrozzo, F.G., Ciarniello, M., Fonte, S., Formisano, M., Frigeri, A., Giardino, M., Longobardo, A., Magni, G., McFadden, L.A., Palomba, E., Pieters, C.M., Tosi, F., Zambon, F., Raymond, C.A., and Russell, C.T. (2017) Localized aliphatic organic material on the surface of Ceres. *Science*, **355**, 719–722.

Dutkiewicz, A., Volk, H., Ridley, J., and George, S. (2003) Biomarkers, brines, and oil in the Mesoproterozoic, Roper Superbasin, Australia. *Geology*, **31**, 981–984.

Ferralis, N., Matys, E.D., Knoll, A.H., Hallmann, C., and Summons, R.E. (2016) Rapid, direct and non-destructive assessment of fossil organic matter *via* microRaman spectroscopy. *Carbon*, **108**, 440–449.

Ganz, H.H. and Kalkreuth, W. (1991) IR classification of kerogen type, thermal maturation, hydrocarbon potential and lithological characteristics. *Journal of Southeast Asian Earth Sciences*, **5**, 19–28.

Goudge, T.A., Russell, J.M., Mustard, J.F., Head, J.W., and Bijaksana, S. (2017) A 40,000 yr record of clay mineralogy at Lake Towuti, Indonesia: Paleoclimate reconstruction from reflectance spectroscopy and perspectives on paleolakes on Mars. *Geological Society of America Bulletin*, **129**, 806–819.

Greenberger, R.N., Mustard, J.F., Ehlmann, B.L., Blaney, D.L., Cloutis, E.A., Wilson, J.H., Green, R.O., and Fraeman, A.A. (2015) Imaging spectroscopy of geological samples and outcrops: Novel insights from microns to meters. *GSA Today*, **25**, 4–10.

Hapke, B. (1993) *Theory of Reflectance and Emittance Spectroscopy*. Cambridge University Press, Cambridge, UK; New York, 513 pp.

Hapke, B. (2008) Bidirectional reflectance spectroscopy. *Icarus*, **195**, 918–926.

Herron, M., Loan, M., Charsky, A., Herron, S.L., Pomerantz, A.E., and Polyakov, M. (2014) Kerogen content and maturity, mineralogy and clay-typeing from DRIFTS analysis of cuttings or core. *Petrophysics*, **55**, 434–446.

Hosterman, J.W., Meyer, R.F., Palmer, C.A., Doughten, M.W., and Anders, D.E. (1989) Chemistry and mineralogy of natural bitumens and heavy oils and their reservoir rocks from the United States, Canada, Trinidad and Tobago, and Venezuela. *United States Geological Survey Circular 1047*.

Izawa, M.R.M., Applin, D.M., Norman, L., and Cloutis, E.A. (2014) Reflectance spectroscopy (350–2500 nm) of solid-state polycyclic aromatic hydrocarbons (PAHs). *Icarus*, **237**, 159–181.

Johnston, D.T., Farquhar, J., Summons, R.E., Shen, Y., Kaufman, A.J., Masterson, A.L., and Canfield, D.E. (2008) Sulfur isotope biogeochemistry of the Proterozoic McArthur Basin. *Geochimica et Cosmochimica Acta*, **72**, 4278–4290.

Kaplan, H.H. and Milliken, R.E. (2016) Reflectance spectroscopy for organic detection and quantification in clay-bearing samples: Effects of albedo, clay type, and water content. *Clays and Clay Minerals*, **64**, 167–184.

Keil, R.G. and Mayer, L.M. (2014) Mineral Matrices and Organic Matter. Pp. 337–359 in: *Treatise on Geochemistry, Vol 12, Reference Module in Earth Systems and Environmental Science (K. Turekian and H. Holland,*

editors), Elsevier.

Leroi, V., Bibring, J.-P., and Berthe, M. (2009) Micromega/IR: Design and status of a near-infrared spectral microscope for *in situ* analysis of Mars samples. *Planetary and Space Science*, **57**, 1068–1075.

Lis, G.P., Mastalerz, M., Schimmelmann, A., Lewan, M.D., and Stankiewicz, B.A. (2005) FTIR absorption indices for thermal maturity in comparison with vitrinite reflectance R0 in type-II kerogens from Devonian black shales. *Organic Geochemistry*, **36**, 1533–1552.

Luo, G., Ono, S., Beukes, N.J., Wang, D.T., Xie, S., and Summons, R.E. (2016) Rapid oxygenation of Earths atmosphere 2.33 billion years ago. *Science Advances*, **2**, e1600134–e1600134.

McCarty, G.W., Reeves, J.B., Reeves, V.B., Follett, R.F., and Kimble, J.M. (2002) Mid-infrared and near-infrared diffuse reflectance spectroscopy for soil carbon measurement. *Soil Science Society of America Journal*, **66**, 640–646.

McCord, T.B., Hansen, G.B., Buratti, B.J., Clark, R.N., Cruikshank, D.P., D'Aversa, E., Griffith, C.A., Baines, E.K.H., Brown, R.H., Dalle Ore, C.M., Filacchione, G., Formisano, V., Hibbitts, C.A., Jaumann, R., Lunine, J.I., Nelson, R.M., and Sotin, C. (2006) Composition of Titan's surface from Cassini VIMS. *Planetary and Space Science*, **54**, 1524–1539.

Mehmani, Y., Burnham, A.K., Vanden Berg, M.D., and Tchelepi, H.A. (2017) Quantification of organic content in shales *via* near-infrared imaging: Green River Formation. *Fuel*, **208**, 337–352.

Milliken, R. and Mustard, J. (2007) Estimating the water content of hydrated minerals using reflectance spectroscopy: I. Effects of darkening agents and low-albedo materials. *Icarus*, **189**, 550–573.

Moroz, L.V., Arnold, G., Korochantsev, A.V., and Wäsch, R. (1998) Natural solid bitumens as possible analogs for cometary and asteroid organics: 1. Reflectance spectroscopy of pure bitumens. *Icarus*, **134**, 253–268.

Mustard, J. and Hays, J. (1997) Effects of Hyperfine Particles on Reflectance Spectra from 0.3 to 25 μm. *Icarus*, **125**, 145–163.

Nash, D.B. and Conel, J.E. (1974) Spectral reflectance systematics for mixtures of powdered hypersthene, labradorite, and ilmenite. *Journal of Geophysical Research*, **79**, 1615–1621.

Nocita, M., Stevens, A., Toth, G., Panagos, P., van Wesemael, B., and Montanarella, L. (2014) Prediction of soil organic carbon content by diffuse reflectance spectroscopy using a local partial least square regression approach. *Soil Biology and Biochemistry*, **68**, 337–347.

Orthous-Daunay, F.-R., Quirico, E., Beck, P., Brissaud, O., Dartois, E., Pino, T., and Schmitt, B. (2013) Mid-infrared study of the molecular structure variability of insoluble organic matter from primitive chondrites. *Icarus*, **223**, 534–543.

Pilorget, C. and Bibring, J.-P. (2013) NIR reflectance hyperspectral microscopy for planetary science: Application to the MicrOmega instrument. *Planetary and Space Science*, **76**, 42–52.

Quirico, E., Moroz, L.V., Schmitt, B., Arnold, G., Faure, M., Beck, P., Bonal, L., Ciarniello, M., Capaccioni, F., Filacchione, G., Erard, S., Leyrat, C., Bockelée-Morvan, D., Zinzi, A., Palomba, E., Drossart, P., Tosi, F., Capria, M.T., De Sanctis, M.C., Raponi, A., Fonti, S., Mancarella, F., Orofino, V., Barucci, A., Blecka, M.I., Carlson, R., Despan, D., Faure, A., Fornasier, S., Gudipati, M.S., Longobardo, A., Markus, K., Mennella, V., Merlin, F., Piccioni, G., Rousseau, B., and Taylor, F. (2016) Refractory and semi-volatile organics at the surface of comet 67P/Churyumov-Gerasimenko: Insights from the Virtis/Rosetta imaging spectrometer. *Icarus*, **272**, 32–47.

Reeves, J.B. (2010) Near- versus mid-infrared diffuse reflectance spectroscopy for soil analysis emphasizing carbon and laboratory versus on-site analysis: Where are we and what needs to be done? *Geoderma*, **158**, 3–14.

Reuter, D.C. and Simon-Miller, A.A. (2012) The OVIRS Visible/IR Spectrometer on the OSIRIS-Rex Mission. Oral presentation on 10/11/2012 in "Instrumentation for *in situ* analysis missions (Venus *in situ* Explorer, Titan, *etc*.) I." session. *International Workshop on Instrumentation for Planetary Missions (IPM-2012), Greenbelt, Maryland, USA*.

Reuter, D.C., Simon, A.A., Hair, J., Lunsford, A., Manthripragada, S., Bly, V., Bos, B., Brambora, C., Caldwell, E., Casto, G., Dolch, Z., Finneran, P., Jennings, D., Jhabvala, M., Matson, E., McLelland, M., Roher, W., Sullivan, T., Weigle, E., Wen, Y., Wilson, D., and Lauretta, D.S. (2018) The OSIRIS-REx Visible and InfraRed Spectrometer (OVIRS): Spectral maps of the asteroid Bennu. *Space Science Reviews*, **214**, 54, https://doi.org/10.1007/s11214-018-0482-9.

Rivard, B., Lyder, D., Feng, J., Gallie, A., Cloutis, E., Dougan, P., Gonzalez, S., Cox, D., and Lipsett, M.G. (2010) Bitumen content estimation of Athabasca oil sand from broad band infrared reflectance spectra. *The Canadian Journal of Chemical Engineering*, **88**, 830–838.

Rivkin, A.S. and Emery, J.P. (2010) Detection of ice and organics on an asteroidal surface. *Nature*, **464**, 1322–1323.

Schopf, J.W. (1983) *Earth's Earliest Biosphere: It's Origin and Evolution*. Princeton University Press, Princeton, NJ, USA, 543 pp.

Speta, M., Rivard, B., Feng, J., Lipsett, M., and Gingras, M. (2015) Hyperspectral imaging for the determination of bitumen content in Athabasca oil sands core samples. *AAPG Bulletin*, **99**, 1245–1259.

Speta, M., Gingras, M.K., and Rivard, B. (2016) Shortwave infrared hyperspectral imaging: A novel method for enhancing the visibility of sedimentary and biogenic features in oil-saturated core. *Journal of Sedimentary Research*, **86**, 830–842.

Sunshine, J.M. and Pieters, C.M. (1993) Estimating modal abundances from the spectra of natural and laboratory pyroxene mixtures using the modified Gaussian model. *Journal of Geophysical Research*, **98**, 9075–9087.

Tosca, N.J., Johnston, D.T., Mushegian, A., Rothman, D.H., Summons, R.E., and Knoll, A.H. (2010) Clay mineralogy, organic carbon burial, and redox evolution in Proterozoic oceans. *Geochimica et Cosmochimica Acta*, **74**, 1579–1592.

van der Meijde, M., Knox, N.M., Cundill, S.L., Noomen, M.F., van der Werff, H.M., and Hecker, C. (2013) Detection of hydrocarbons in clay soils: A laboratory experiment using spectroscopy in the mid- and thermal infrared. *International Journal of Applied Earth Observation and Geoinformation*, **23**, 384–388.

Vohland, M., Besold, J., Hill, J., and Fründ, H.-C. (2011) Comparing different multivariate calibration methods for the determination of soil organic carbon pools with visible to near infrared spectroscopy. *Geoderma*, **166**, 198–205.

Washburn, K.E., Birdwell, J.E., Foster, M., and Gutierrez, F. (2015) Detailed description of oil shale organic and mineralogical heterogeneity *via* Fourier transform infrared microscopy. *Energy & Fuels*, **29**, 4262–4271.

(*Received 23 October 2017; revised 7 April 2018; Ms. 1231; AE: M. Plötze*)